

Lattice dynamics of K_2NaAlF_6 , K_3AlF_6 , and Na_3AlF_6 crystals with the elpasolite structure

V. I. Zinenko^{*)} and N. G. Zamkova

L. V. Kirenskii Physics Institute Siberian Section, Russian Academy of Sciences, 660036 Krasnoyarsk, Russia

S. N. Sofronova

Krasnoyarsk State University, 660041 Krasnoyarsk, Russia

(Submitted 11 March 1998)

Zh. Éksp. Teor. Fiz. **114**, 1742–1756 (November 1998)

This paper presents the results of a nonempirical calculation of the static and dynamic properties of K_2NaAlF_6 , K_3AlF_6 , and Na_3AlF_6 crystals with the elpasolite structure. The calculation is based on a microscopic model of an ionic crystal that allows for the deformability and polarizability of the ions. The deformability parameters of the ions are determined by minimizing the total energy of the crystal. The total energy is regarded as a functional of the electron density, using the local Thomas–Fermi approximation and taking into account exchange (correlation) effects. The results of the calculations of the equilibrium lattice parameters and of the permittivities are in good agreement with the experimental data. Unstable vibrational modes are found in the spectrum of the lattice vibrations, with these modes occupying the phase space in the entire Brillouin zone. © 1998 American Institute of Physics. [S1063-7761(98)01311-0]

1. INTRODUCTION

The family of crystals with the elpasolite structure $A_2BB^{3+}X_6$ can be classified as perovskite-like compounds, a typical structural feature of which is the presence of octahedral groups. Most crystals of this family, like the representatives of the perovskite family, experience diverse structural phase transitions associated with instability of the crystal lattice against various vibrational lattice modes.

Crystals of the elpasolite family in the high-symmetry phase belong to the cubic space group O_h^5 , with a face-centered lattice. The unit cell contains one molecule. Depending on the chemical composition, various distorted low-symmetry phases are observed, with sequences of structural phase transitions being detected in many crystals of this family.

Compounds with the elpasolite structure have been intensively studied by various methods, and by now there is much experimental information for many crystals of the given family concerning the structures, the physical properties, and their changes during phase transformations. In particular, Raman scattering and inelastic neutron scattering in certain crystals have been used to determine the soft vibrational modes of the crystal lattice.¹ The experimental data on the structures of the low-symmetry phases and the soft modes of the lattice vibrations are evidence that, in most of the compounds of the elpasolite family that have been studied, the phase transitions are associated with small rotations of the $B^{3+}X_6$ octahedra. However, it is also experimentally known that the structures of the distorted phases in certain elpasolites correspond not only to rotations of the octahedra, but also to substantial displacements of the A and B ions from the equilibrium positions of the cubic phase. There

have been virtually no calculations of the frequency spectrum of the lattice vibrations in crystals of the elpasolite family. Such a calculation of the incomplete vibrational spectrum of the $Cs_2NaTmBr_6$ crystal in the rigid-ion model is given in Ref. 1. Since the unit cell of elpasolite contains ten atoms, a large number of unknown parameters are needed in the rigid-ion model to take into account short-range forces (Ref. 1 used nine parameters). For this reason, it is difficult to use the rigid-ion model to study the crystal lattice's instability against one vibrational mode or another as a function of the chemical composition of the compounds.

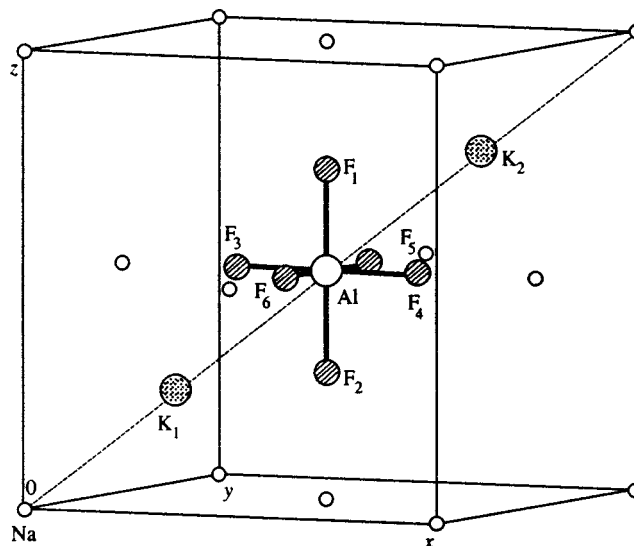


FIG. 1. Structure of the elpasolite K_2NaAlF_6 . One molecule and the face-centered Na lattice are shown.

The goal of this paper is to calculate from first principles the equilibrium volume, the total spectrum of the lattice vibrations, and the radio-frequency (rf) permittivity in K_2NaAlF_6 , K_3AlF_6 , and Na_3AlF_6 crystals in terms of the generalized Gordon–Kim model proposed by Ivanov and Maksimov.²

Section 2 presents the results of a group-theoretical analysis of the normal modes of the lattice vibrations of the elpasolite structure for all symmetry points and directions of the Brillouin zone. The results of such an analysis appear in the literature for only two symmetry points (Γ and X) of the Brillouin zone.^{1,3} The model and the method of computing the frequencies of the lattice normal modes and the rf permittivity are presented in Sec. 3. The results of the calculations and a discussion of the results are presented in Sec. 4.

2. SYMMETRY ANALYSIS OF THE NORMAL MODES

The crystal structure of elpasolite in the high-symmetry phase is cubic with space group $O_h^5(Fm\bar{3}m)$. The ions occupy ten interpenetrating fcc lattices, as shown in Fig. 1.

The characters of the various symmetry elements in the vibrational representation are as follows (only the symmetry elements associated with the z direction are shown below, $\tau = a_0/2$, and a_0 is the lattice parameter):

the identity element

$$\chi(E) = 30,$$

rotation about a fourfold axis

$$\chi(C_{4z}) = 1 + 3\exp(i\mathbf{q} \cdot (2\tau, 0, 0)),$$

rotation about a twofold axis

$$\chi(C_{2z}) = (-1)[1 + 3\exp(i\mathbf{q} \cdot (2\tau, 2\tau, 0)) + \exp(i\mathbf{q} \cdot (\tau, \tau, 0)) + \exp(i\mathbf{q} \cdot (3\tau, 3\tau, 0))],$$

rotation about a twofold axis along a face diagonal

$$\chi(C_{2xy}) = (-1)[1 + \exp(i\mathbf{q} \cdot (2\tau, 2\tau, 2\tau))],$$

reflection in a plane perpendicular to a twofold axis

$$\chi(C_{\sigma_z}) = 1 + 5\exp(i\mathbf{q} \cdot (0, 0, 2\tau)),$$

reflection in a plane perpendicular to a face diagonal

$$\chi(C_{\sigma_{xy}}) = 1 + 3\exp(i\mathbf{q} \cdot (2\tau, 2\tau, 0)) + \exp(i\mathbf{q} \cdot (\tau, \tau, 0)) + \exp(i\mathbf{q} \cdot (3\tau, 3\tau, 0)),$$

TABLE I. Displacements of ions of an elpasolite in the normal modes of the center and of boundary point X of the Brillouin zone.

Irreducible representation	Normal mode	Number of modes
Zone center		
A_{1g}	$-F_{1z} = F_{2z} = -F_{3y} = F_{4y} = F_{5x} = -F_{6x}$	1
E_g	$-F_{1z} = -F_{2z} = F_{3y} = F_{4y} = -F_{5x} = F_{6x}$ $-F_{1z} = F_{2z} = F_{3x} = -F_{4x} = F_{5y} = F_{6y}$	1
T_{1g}	$-F_{1y} = F_{2y} = F_{5z} = -F_{6z}$ $-F_{1x} = F_{2x} = -F_{3z} = F_{4z}$ $-F_{3y} = F_{4y} = -F_{5x} = F_{6x}$	1
T_{2g}	$K_{1x} = K_{1y} = K_{1z} = -K_{2x} = -K_{2y} = -K_{2z};$ $-F_{1x} = -F_{1y} = F_{2x} = F_{2y} = F_{3y} = F_{3z} = -F_{4y} = -F_{4z}$ $= -F_{5x} = -F_{5z} = F_{6x} = F_{6z}$ $K_{1x} = -K_{2x}; -K_{1y} = K_{2y}; K_{1z} = K_{2z};$ $F_{1x} = -F_{2x} = -F_{3z} = F_{4z};$ $-F_{1y} = F_{2y} = F_{5z} = F_{6z}; F_{3y} = -F_{4y} = -F_{5x} = F_{6x}$ $K_{1x} = -K_{2x}; K_{1y} = -K_{2y}; -K_{1z} = K_{2z};$ $-F_{1y} = F_{2y} - F_{5z} = F_{6z};$ $-F_{1y} = F_{2y} = -F_{5z} = F_{6z}; -F_{3y} = F_{4y} = F_{5x} = -F_{6x}$	2
T_{2u}	$F_{1y} = F_{2y} = -F_{5y} = -F_{6y}$ $F_{1x} = F_{2x} = -F_{3x} = -F_{4x}$ $F_{3z} = F_{4z} = -F_{5z} = -F_{6z}$	1
T_{1u}	all ions are displaced	4
point X		
τ_3	$F_{3y} = -F_{4y} = F_{5x} = -F_{6x}$	1
τ_5	$F_{3x} = -F_{4x} = F_{5y} = -F_{6y}$	1
τ_7	$F_{3y} = -F_{4y} = -F_{5x} = F_{6x}$	1
τ_8	$F_{3z} = F_{4z} = -F_{5z} = -F_{6z}$	1
τ_6	$K_{1z} = -K_{2z}$	1
τ_1	all ions are displaced	3
τ_9	all ions are displaced	3
τ_{10}	all ions are displaced	6

inversion

$$\chi(J) = (-3)[1 + \exp(i\mathbf{q} \cdot (2\tau, 2\tau, 2\tau))],$$

inverted rotation by 60°

$$\chi(S_6) = 0,$$

inverted rotation by 90°

$$\chi(S_{4z}) = (-1)[1 + \exp(i\mathbf{q} \cdot (0, 2\tau, 2\tau)) + \exp(i\mathbf{q} \cdot (0, \tau, \tau)) + \exp(i\mathbf{q} \cdot (0, 3\tau, 3\tau))].$$

The expansion of the modal representation T into irreducible representations can be found by the standard procedure:⁴

$$C_\lambda = n^{-1} \sum_g \chi(\mathbf{q}, g) \chi^\lambda(\mathbf{q}, g), \quad (1)$$

where n is the order of the group of wave vector \mathbf{q} , and $\chi^\lambda(\mathbf{q}, g)$ is the character of the small representation of the group of vector \mathbf{q} . This decomposition has the following form for the symmetry points and directions of the Brillouin zones of the fcc lattice (the symbols for the wave vectors and irreducible representations are from Kovalev's tables;⁵ for the zone center, the standard symbols for the representations of the space groups are shown in parentheses):

(a) Center of the Brillouin zone, $\mathbf{q} = (0, 0, 0)$

$$T = \tau_1(A_{1g}) + \tau_3(E_g) + \tau_5(T_{1g}) + 2\tau_4(T_{2g}) + \tau_9(T_{2u}) + 5\tau_{10}(T_{1u}).$$

Here the splitting of the longitudinal and transverse optical frequencies of symmetry T_{1u} by the macroscopic electric field is neglected.

(b) $\mathbf{q} = (0, 0, 2\mu\pi/\tau)$

$$T = 7\tau_1 + \tau_2 + 2\tau_3 + 2\tau_4 + 9\tau_5.$$

The mode with symmetry τ_5 is doubly degenerate. At the zone boundary (point X),

$$T = 3\tau_1 + \tau_3 + 4\tau_4 + \tau_5 + \tau_6 + \tau_7 + \tau_8 + 3\tau_9 + 6\tau_{10},$$

τ_9 and τ_{10} correspond to doubly degenerate modes.

(c) $\mathbf{q} = (2\mu\pi/\tau, 2\mu\pi/\tau, 0)$ (point K corresponds to $\mathbf{q} = (3\pi/4\tau, 3\pi/4\tau, 0)$)

$$T = 10\tau_2 + 4\tau_2 + 8\tau_3 + 8\tau_4.$$

(d) $\mathbf{q} = (\mu\pi/\tau, \mu\pi/\tau, \mu\pi/\tau)$

$$T = 8\tau_1 + 2\tau_2 + 10\tau_3,$$

τ_3 corresponds to doubly degenerate modes. At the zone boundary (point L),

$$T = 4\tau_1 + \tau_2 + \tau_3 + 4\tau_4 + 5\tau_5 + 5\tau_6,$$

τ_5 and τ_6 correspond to doubly degenerate modes.

(e) $\mathbf{q} = (0, \pi/\tau, \pi/2\tau)$ (point W)

$$T = 5\tau_1 + 2\tau_2 + 5\tau_3 + 2\tau_4 + 8\tau_5,$$

τ_5 corresponds to doubly degenerate modes.

The displacements of the ions in certain normal modes are given in Table I.

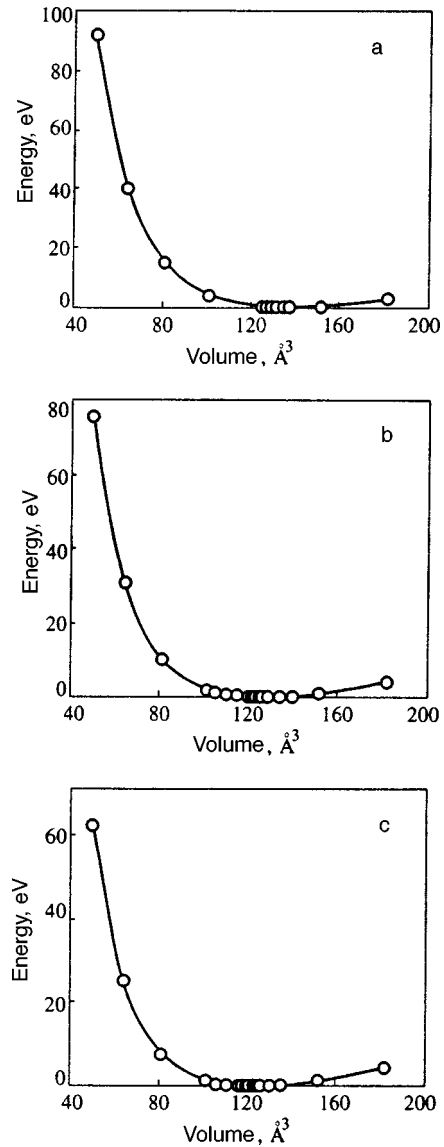


FIG. 2. Dependence of the total energy of the crystal on the volume: (a) K_3AlF_6 ; (b) K_2NaAlF_6 ; (c) Na_3AlF_6 . The origin of the energy readings in (a), (b), and (c) corresponds to 72 784 eV, 60 751 eV, and 36 683 eV.

3. MODEL. METHOD OF CALCULATION

The model of the ionic crystal proposed by Ivanov and Maximov,² which takes into account the polarizability of the ions, is used to compute the frequency spectrum of the lattice vibrations of crystals of the elpasolite family. In this model, the ionic crystal is represented as consisting of individual intersecting spherically symmetric ions. The total electron density of the crystal in this case can be written

$$\rho(\mathbf{r}) = \sum_i \rho_i(\mathbf{r} - \mathbf{R}_i),$$

where symmetrization is carried out over all the ions of the crystal.

The total energy of the crystal in terms of the density-functional method, taking into account only pairwise interaction, has the form

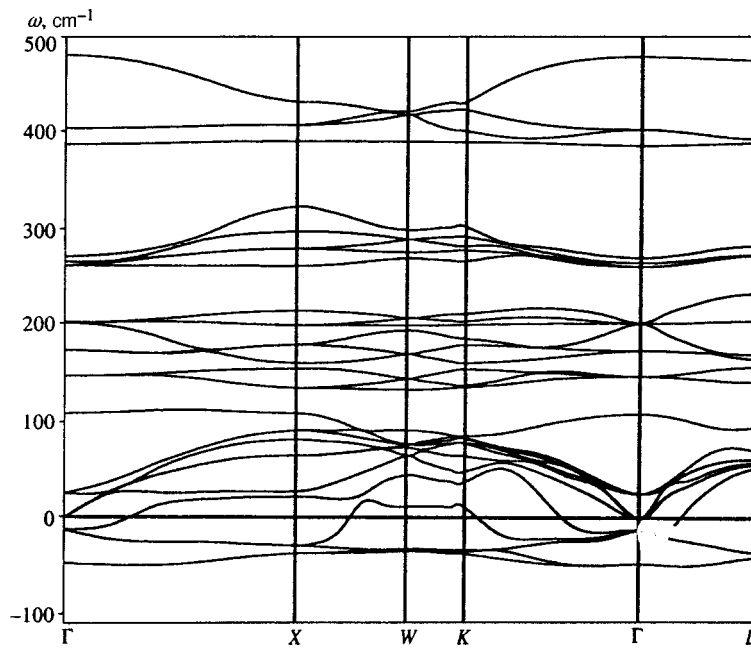


FIG. 3. Calculated dispersion curves for cubic K_2NaAlF_6 . (Imaginary frequencies are indicated by negative values.)

$$E_{cr} = \frac{1}{2} \sum_{i \neq j} \frac{Z_i Z_j}{|\mathbf{R}_i - \mathbf{R}_j|} + \sum_i E_i^{self}(R_w^i) + \frac{1}{2} \sum_{i \neq j} \Phi_{ij}(R_w^i, R_w^j, |\mathbf{R}_i - \mathbf{R}_j|), \quad (2)$$

where Z_i is the charge of the i th ion,

$$\Phi_{ij}(R_w^i, R_w^j, |\mathbf{R}_i - \mathbf{R}_j|) = \mathbf{E}\{\rho_i(\mathbf{r} - \mathbf{R}_i) + \rho_j(\mathbf{r} - \mathbf{R}_j)\} - \mathbf{E}\{\rho(\mathbf{r} - \mathbf{R}_i)\} - \mathbf{E}\{\rho(\mathbf{r} - \mathbf{R}_j)\}, \quad (3)$$

energy $\mathbf{E}\{\rho\}$ is calculated by the density-functional method,²

using the local approximation for the kinetic and exchange (correlation) energies, and $E_i^{self}(R_w^i)$ is the self-energy of the ion. The electron density of an individual ion and its self-energy are calculated taking into account the crystal potential, approximated by a charged sphere (the Watson Sphere)

$$v(r) = \begin{cases} Z_i^{ion}/R_w, & r < R_w \\ Z_i^{ion}/r, & r > R_w \end{cases}$$

where R_w is the radius of the Watson sphere. The radii R_w^i of the spheres at individual ions are found by minimizing the total energy of the crystal.

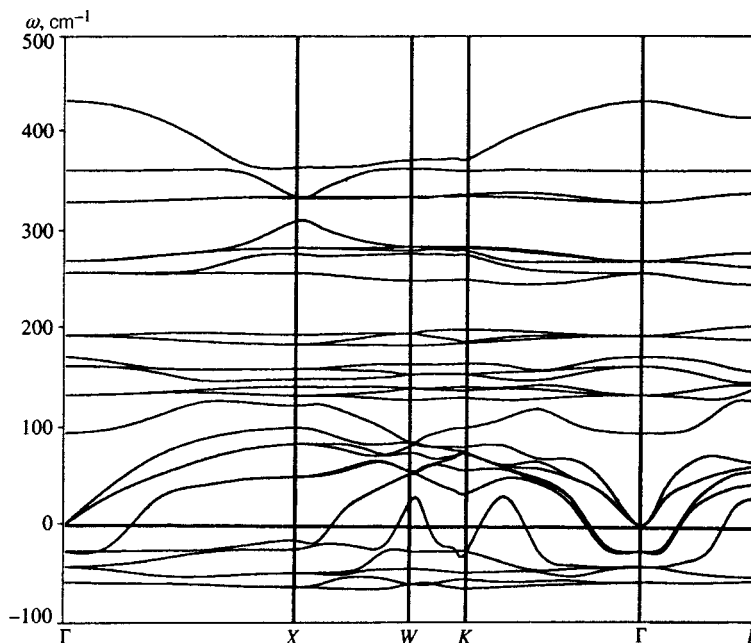


FIG. 4. Calculated dispersion curves for cubic K_3AlF_6 . (Imaginary frequencies are indicated by negative values.)

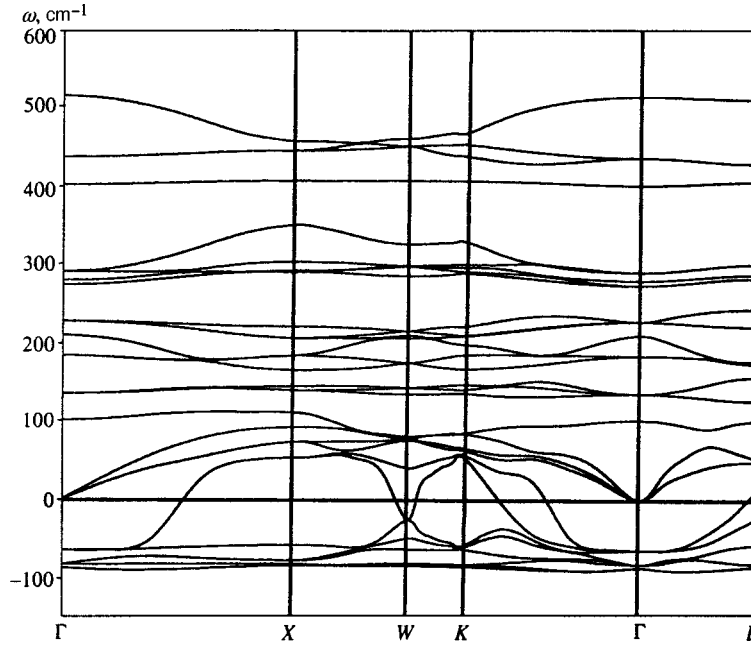


FIG. 5. Calculated dispersion curves for cubic Na₃AlF₆. (Imaginary frequencies are indicated by negative values.)

To calculate the lattice dynamics in the expression for the energy of the crystal, Eq. (2), it is necessary to add terms that describe the energy changes caused by displacing the ions from their equilibrium positions. When the frequencies of the lattice vibrations of the ionic crystals were calculated, the electronic polarizability of the ions and the “breathing” of the ion in the crystal environment were taken into account both in terms of the phenomenological models of Ref. 6 and the microscopic approach of Ref. 7. In the model considered here, the expression for the dynamic matrix has the form

$$\begin{aligned}
 D_{jj'}^{\alpha\beta} = & \frac{\exp(-i\mathbf{q}(\mathbf{x}_j - \mathbf{x}_{j'}))}{\sqrt{M_j M_{j'}}} \left\{ \frac{1}{2} Z_j^{\text{ion}} Q^{\alpha\beta}(\mathbf{q}; jj') Z_{j'}^{\text{ion}} \right. \\
 & + \Phi_{RR}^{\alpha\beta}(\mathbf{q}; jj') + \sum_{k=1}^N [\Phi_{Rv}^{\alpha}(\mathbf{q}; jk) V^{\beta}(\mathbf{q}; kj')] \\
 & + V^{*\alpha}(\mathbf{q}; kj) \Phi_{vR}^{\beta}(\mathbf{q}; kj')] \\
 & + \sum_{k, k'=1}^N V^{*\alpha}(\mathbf{q}; kj) \Phi_{vv}(\mathbf{q}; kk') V^{\beta}(\mathbf{q}; k'j') \\
 & + \sum_{\gamma=1}^3 \sum_{k=1}^N [W^{*\gamma\alpha}(\mathbf{q}; kj) \Phi_{wR}^{\gamma\beta}(\mathbf{q}; jk) \\
 & + \Phi_{Rw}^{\alpha\gamma}(\mathbf{q}; jk) W^{\gamma\beta}(\mathbf{q}; kj')] + \sum_{\gamma, \gamma'=1}^3 \sum_{k, k'=1}^N W^{*\gamma\alpha} \\
 & \times (\mathbf{q}; kj) \Phi_{ww}^{\gamma, \gamma'}(\mathbf{q}; kk') W^{\gamma'\beta}(\mathbf{q}; k'j') \\
 & + \sum_{\gamma=1}^3 \sum_{k, k'=1}^N [W^{*\gamma\alpha}(\mathbf{q}; kj) \Phi_{wv}^{\gamma}(\mathbf{q}; kk') V^{\beta}(\mathbf{q}; k'j') \\
 & \left. + V^{*\alpha}(\mathbf{q}; kj) \Phi_{wv}^{\gamma}(\mathbf{q}; kk') W^{\gamma\beta}(\mathbf{q}; k'j')] \right\}, \quad (4)
 \end{aligned}$$

where N is the number of atoms per unit cell, \mathbf{x}_j are the coordinates of atom j inside the unit cell, and $Q^{\alpha\beta}(\mathbf{q}; jj')$ is the contribution to the dynamic matrix from long-range Coulomb interactions. The matrices entering into Eq. (4) have the form

$$\hat{V} = -\hat{\Phi}_{vv}^{-1} \hat{P}_{vR}, \quad \hat{W} = \hat{R}_{ww}^{-1} \hat{\Phi}_{ww}^{-1} \hat{S}_{wR},$$

$$\hat{R}_{ww} = 1 - \hat{\Phi}_{ww}^{-1} \hat{\Phi}_{wv} \hat{\Phi}_{vv}^{-1}, \quad \hat{S}_{wR} = \hat{\Phi}_{wv} \hat{\Phi}_{vv}^{-1} \hat{\Phi}_{vR} - \hat{\Phi}_{wR},$$

$$\hat{P}_{vR} = \hat{\Phi}_{vR} + \hat{\Phi}_{vW} \hat{R}_{ww}^{-1} \hat{\Phi}_{ww}^{-1} \hat{S}_{wR}.$$

The matrix $\hat{\Phi}$ is defined as

$$\Phi_{RR}^{\alpha\beta}(\mathbf{q}; jj') = \sum_{\Gamma} \frac{\partial^2 \Phi(\mathbf{1}0)}{\partial R_{\alpha}(\mathbf{j}) \partial R_{\beta}(\mathbf{j}')} \exp(-i\mathbf{q}\mathbf{l}),$$

$$\Phi_{vv}(\mathbf{q}; jj') = \sum_{\Gamma} \frac{\partial^2 \Phi(\mathbf{j}\mathbf{j}')}{\partial v_j \partial v_{j'}} \exp(-i\mathbf{q}\mathbf{l}),$$

$$\Phi_{ww}^{\alpha\beta}(\mathbf{q}; jj') = Q^{\alpha\beta}(\mathbf{q}; jj') + \Gamma^{\alpha\beta}(\mathbf{q}; jj') + \frac{\delta_{jj'} \delta_{\alpha\beta}}{\alpha_j}, \quad (5)$$

$\Gamma^{\alpha\beta}(\mathbf{q})$ is the matrix of the short-range part of the dipole-dipole interaction, α_j is the polarizability of the j th ion,

TABLE II. Equilibrium values of the lattice parameters, the polarizabilities of the ions, and the rf permittivities.

Crystal	Model	$a_0, \text{Å}$		Polarizability, Å^3					ϵ_∞	
		Calc.	Exp.	$\alpha_{K'}$	α_K	α_{Na}	α_{Al}	α_F	Calc.	Exp.
K_2NaAlF_6	I	8.12	8.11(Ref. 9)							
	II	8.12			0.696	0.122	0.034	1.123	2.27	1.79(Ref. 9)
	III	7.94								
	IV	7.94			0.836	0.122	0.034	0.720	1.80	
K_3AlF_6	I	8.20	8.38(Ref. 9)							
	II	8.20		0.696	0.696		0.034	1.123	2.23	1.80(Ref. 9)
	III	8.12								
	IV	8.12		0.726	0.836		0.034	0.749	1.86	
Na_3AlF_6	I	8.09	7.95(Ref. 10)							
	II	8.09				0.122	0.034	1.123	2.05	1.78(Ref. 9)
	III	7.86								
	IV	7.86				0.122	0.034	0.720	1.61	

$$\begin{aligned} \Phi_{Rv}^\alpha(\mathbf{q};jj') &= \sum_{\mathbf{l}} \frac{\partial^2 \Phi \left(\begin{smallmatrix} \mathbf{10} \\ jj' \end{smallmatrix} \right)}{\partial R_\alpha \left(\begin{smallmatrix} \mathbf{1} \\ j \end{smallmatrix} \right) \partial v_{j'}} \exp(-i\mathbf{q}\mathbf{l}), \\ \Phi_{vR}^\beta(\mathbf{q};jj') &= \sum_{\mathbf{l}} \frac{\partial^2 \Phi \left(\begin{smallmatrix} \mathbf{10} \\ jj' \end{smallmatrix} \right)}{\partial v_j \partial R_\beta \left(\begin{smallmatrix} \mathbf{0} \\ j' \end{smallmatrix} \right)} \exp(-i\mathbf{q}\mathbf{l}), \\ \Phi_{wR}^{\alpha\beta}(\mathbf{q};jj') &= \sum_{\mathbf{l}} \frac{\partial E_\alpha^{\text{sh}} \left(\begin{smallmatrix} \mathbf{10} \\ jj' \end{smallmatrix} \right)}{\partial R_\beta \left(\begin{smallmatrix} \mathbf{0} \\ j' \end{smallmatrix} \right)} \exp(-i\mathbf{q}\mathbf{l}), \\ \Phi_{wv}^\alpha(\mathbf{q};jj') &= \sum_{\mathbf{l}} \frac{\partial E_\alpha^{\text{sh}} \left(\begin{smallmatrix} \mathbf{10} \\ jj' \end{smallmatrix} \right)}{\partial v_{j'}} \exp(-i\mathbf{q}\mathbf{l}), \\ \Phi_{vw}^\beta(\mathbf{q};jj') &= \sum_{\mathbf{l}} \frac{\partial E_\beta^{\text{sh}} \left(\begin{smallmatrix} \mathbf{10} \\ jj' \end{smallmatrix} \right)}{\partial v_j} \exp(-i\mathbf{q}\mathbf{l}), \\ \hat{\Phi}_{Rw} &= \hat{\Phi}_{wR}^+, \end{aligned} \tag{6}$$

and \mathbf{E}^{sh} is the short-range crystal field created at the j th ion. The expression for the rf permittivity ϵ_∞ can be written

$$\epsilon_\infty^{\alpha\beta} = \delta_{\alpha\beta} + \frac{4\pi q_\alpha}{q^2} \sum_{\gamma=1}^3 \sum_{k,k'=1}^N q_\gamma [\Phi_{wv}^{-1}]^{\gamma\beta}(0;kk').$$

The Coulomb contribution to the dynamic matrix $Q^{\alpha\beta}(\mathbf{q};jj')$ was calculated by the Ewald method. The calculation for the ion was carried out according to Liberman's program,⁸ and the energy of the pairwise interaction from Eq. (3) and the polarizability of the ion were calculated according to Ivanov and Maksimov's program,² using the Thomas–Fermi approximation for the kinetic energy and the Hedin–Lundquist approximation for the exchange energy. The technique of approximating the dependences of the energy on the distance \mathbf{R} and the potentials v of the Watson sphere was used to compute the partial derivatives in Eqs. (5)

and (6), entering into the dynamic matrix of Eq. (4). Chebyshev polynomials were used for the approximations.²

4. RESULTS AND DISCUSSION

This section presents the results of calculations of the total energy, the equilibrium volume, and the lattice vibration spectra for three crystals and four models. The calculations in Model I use the electron density of free spherically symmetrical ions (the rigid-ion model). Model II takes into account the polarizability of the ions. In Model III, the effect of the crystal environment is taken into account by using the potential of the Watson sphere when calculating the electron density of the ions. For simplicity, we used the Watson-sphere potential for only two types of ions in the crystals under discussion: for the K^+ ion and the F^- ion. As shown by our estimates for Al^{3+} and Na^+ ions, the electron density of the free ions is virtually the same as the electron density of these ions in the Watson sphere. Finally, Model IV takes into account the deformability and polarizability of the ions.

TABLE III. Limiting frequencies of the ($q=0$) vibrations of K_2NaAlF_6 .

ω_i (cm^{-1})	Degeneracy	Type of vibration	Models			
			I	II	III	IV
ω_1^L	1	T_{1u}	537.9	435.7	558.5	478.6
ω_2^T	2	T_{1u}	399.3	380.2	427.5	403.2
ω_3	1	A_{1g}	394.9	268.9	456.4	386.6
ω_4^L	1	T_{1u}	299.5	194.9	359.4	270.5
ω_5^T	2	T_{1u}	279.1	194.8	356.6	265.5
ω_6	2	E_g	227.5	226.8	268.0	261.4
ω_7^L	1	T_{1u}	197.9	176.0	213.5	202.5
ω_8	3	T_{2g}	264.7	148.0	308.6	202.1
ω_9^T	2	T_{1u}	150.3	146.0	178.8	173.6
ω_{10}	3	T_{2u}	117.8	96.3	166.0	146.8
ω_{11}^L	1	T_{1u}	124.0	102.9	120.8	108.3
ω_{12}	3	T_{1g}	37.7i	37.7i	30.2	25.1
ω_{13}	3	T_{1u}	0.0	0.0	0.0	0.0
ω_{14}	3	T_{2g}	88.8	73.5i	70.7	12.1i
ω_{15}^T	2	T_{1u}	87.8	46.7i	61.1	47.0i

TABLE IV. Limiting frequencies of the ($q=0$) vibrations of K_3AlF_6 .

ω_i (cm^{-1})	Degeneracy	Type of vibration	Models			
			I	II	III	IV
ω_1^L	1	T_{1u}	489.9	385.0	517.8	432.8
ω_2^T	2	T_{1u}	297.8	381.3	329.4	349.5
ω_3	1	A_{1g}	377.5	268.6	432.9	361.4
ω_4^L	1	T_{1u}	314.8	247.9	352.2	269.8
ω_5^T	2	T_{1u}	305.4	241.5	350.1	269.7
ω_6	2	E_g	229.4	229.1	260.6	257.7
ω_7^L	1	T_{1u}	175.5	143.8	188.9	172.3
ω_8	3	T_{2g}	249.0	150.6	287.6	193.8
ω_9^T	2	T_{1u}	166.6	143.8	171.3	162.4
ω_{10}	3	T_{2u}	109.9	93.1	148.4	132.8
ω_{11}^L	1	T_{1u}	117.2	74.8	112.5	94.2
ω_{12}	3	T_{1g}	31.6i	31.6i	24.7i	26.6i
ω_{13}	3	T_{1u}	0.0	0.0	0.0	0.0
ω_{14}	3	T_{2g}	66.2	85.1i	53.5	42.3i
ω_{15}^T	2	T_{1u}	58.8	69.6i	38.8	58.2i

The results of the calculations are shown in Figs. 2–5 and in Tables II–V. The equilibrium values of the lattice parameters were determined by minimizing the total energy of the crystal as a function of volume (Fig. 2). The lattice parameters are shown in Table II along with the experimental values. For all three materials, the calculated lattice parameters agree with the experimental data to within 2%. The radii of the Watson spheres for the K^+ and F^- ions, found by minimizing the total energy, are 2.0 au and 2.2–2.3 au, respectively.

Table II shows the calculated polarizabilities of the ions and the rf permittivities of the materials under consideration. This table also shows the experimental values of ϵ_∞ . As can be seen from the table, the calculated polarizabilities of the fluorine ions are substantially different in the free-ion approximation (and taking into account the crystal environment within the Watson sphere), and this in turn results in a difference in the calculated rf permittivities for all three materials.

The calculated dispersion curves of the frequencies of the lattice vibrations for the three compounds are shown in Figs. 3–5. In order not to clutter the figures, we show in them the calculated results only for Model IV, since the $\omega(\mathbf{q})$ dependences are qualitatively the same for all four models, while the quantitative differences in the frequencies of the lattice vibrations calculated in Models I–IV are shown in Tables III–V, which display the limiting frequencies of the ($q=0$) vibrations. As can be seen from Figs. 3–5 and Tables II–IV, there are imaginary frequencies of the lattice vibrations in all compounds under discussion; this is evidence of structural instability of the cubic phase in these materials. It should be emphasized that the unstable modes occupy all the phase space in the Brillouin zone. In the K_3AlF_6 and Na_3AlF_6 crystals, there is instability of the structure in all four models. In the K_2NaAlF_6 crystal, the cubic phase is stable at zero temperature only in the model of the deformed ion that neglects polarizability. As can be seen

TABLE V. Limiting frequencies of the ($q=0$) vibrations of Na_3AlF_6 .

ω_i (cm^{-1})	Degeneracy	Type of vibration	Models			
			I	II	III	IV
ω_1^L	1	T_{1u}	487.9	380.1	579.3	513.5
ω_2^T	2	T_{1u}	349.5	305.3	454.1	435.9
ω_3	1	A_{1g}	335.6	215.6	480.6	400.8
ω_4^L	1	T_{1u}	257.7	191.9	372.9	280.2
ω_5^T	2	T_{1u}	248.4	190.0	366.0	274.0
ω_6	2	E_g	151.0	149.0	294.1	291.0
ω_7^L	1	T_{1u}	171.5	154.5	221.6	210.4
ω_8	3	T_{2g}	258.3	170.3	314.5	227.9
ω_9^T	2	T_{1u}	123.2	114.4	188.7	184.3
ω_{10}	3	T_{2u}	98.8	85.2	147.4	135.6
ω_{11}^L	1	T_{1u}	70.3	34.0	116.7	101.9
ω_{12}	3	T_{1g}	57.6i	58.5i	81.9i	82.1i
ω_{13}	3	T_{1u}	0.0	0.0	0.0	0.0
ω_{14}	3	T_{2g}	81.6i	95.3i	80.9i	64.4i
ω_{15}^T	2	T_{1u}	90.7i	96.4i	58.1i	86.4i

from Tables III–V, taking the polarizability of the ions into account in all the compounds under consideration reduces almost all the frequencies of the lattice vibrations, increases the number of unstable modes, and appreciably reduces the splitting of the longitudinal and transverse vibrational frequencies of the polar modes.

It can be seen from Figs. 3–5 and Tables III–V that the cubic phase in the compounds under consideration is most unstable in the Na_3AlF_6 crystal and most stable in K_2NaAlF_6 . This conclusion qualitatively agrees with the results of experimental studies of structural phase transitions in these crystals.⁹ It has been established that the phase-transition temperature in Na_3AlF_6 significantly exceeds the transition temperature in K_3AlF_6 , while no phase transitions are detected in the K_2NaAlF_6 crystal up to liquid-nitrogen temperatures.

There are three types of instability of the cubic structure at the center of the Brillouin zone. One is the ferroelectric instability associated with transverse vibrations of the polar mode T_{1u} . In this mode, all the atoms in a unit cell are displaced from the equilibrium positions of the cubic phase. Ferroelectric phase transitions, as far as we know, have not been experimentally observed in halide crystals with the elpasolite structure. Another instability is associated with the triply degenerate T_{1g} mode.

Only the four fluorine atoms are displaced from the equilibrium positions in this mode, and these displacements cause the AlF_6 octahedron to rotate as a whole (see Table I). Finally, a third type of instability is associated with the triply degenerate T_{2g} mode. In one of the eigenvectors of this mode, the displacements of the atoms cause the AlF_6 octahedron to rotate about the body diagonal while the potassium (sodium) atoms located on that diagonal are simultaneously displaced toward each other. Note that there is another, stable mode with the same T_{2g} symmetry in the vibrational spectrum of the crystals under consideration (see Tables III–V).

5. CONCLUSION

The static and dynamic properties of three crystals with the elpasolite structure have thus been calculated in this paper in terms of a simple nonempirical model of an ionic crystal. The calculated equilibrium values of the lattice parameters and the permittivity are in good agreement with the experimental data. Unfortunately, we cannot compare the calculated frequencies of the lattice vibrations with measured results, since such measurements have apparently not been made for the crystals considered here. Our results concerning the instability of the cubic structure and the presence of unstable modes in a large phase space of the Brillouin zone are apparently common to crystals with the given structure.

The authors are grateful to the Russian Fund for Fundamental Research (Projects 97-02-16277 and 96-15-96700) for financial support of this work. We are grateful to O. V. Ivanov and E. G. Maksimov for allowing us to use their programs to calculate the total energy and polarizability of the ions.

*⁹E-mail: zinenko@ph.krasnoyarsk.su

- ¹W. Bührer and H. U. Güdel, *J. Phys. C* **20**, 3809 (1987).
- ²O. V. Ivanov and E. G. Maksimov, *Zh. Éksp. Teor. Fiz.* **108**, 1841 (1995) [*JETP* **81**, 1008 (1995)].
- ³M. Couzi, S. Khairoun, and A. Tressand, *Phys. Status Solidi A* **98**, 423 (1986).
- ⁴A. A. Maradudin and V. Vosko, *Rev. Mod. Phys.* **40**, 1 (1968).
- ⁵O. V. Kovalev, *Irreducible Representations of the Space Groups*, Gordon & Breach, New York (1965).
- ⁶V. Nüsslein and U. Schröder, *Phys. Status Solidi* **21**, 309 (1967).
- ⁷A. Chizmeshya, F. M. Zimmermann, R. A. LaViolette, and G. H. Wolf, *Phys. Rev.* **50**, 15 559 (1994).
- ⁸D. A. Liberman, D. T. Cromer, and J. J. Waber, *Comput. Phys. Commun.* **2**, 107 (1971).
- ⁹*Minerals. A Collection*, vol. 2, Akad. Nauk SSSR, Moscow (1963).
- ¹⁰H. Bode and E. Voss, *Z. Anorg. Allg. Chem.* **200**, 1 (1957).

Translated by W. J. Manthey